

APPLICATION OF DIGITAL TWIN CONCEPT FOR SUPERCRITICAL CO₂ OFF-DESIGN
PERFORMANCE AND OPERATION ANALYSES

Leonid Moroz¹, Maksym Burlaka¹, Tishun Zhang¹, Olga Altukhova¹

¹SoftInWay Inc., Burlington, MA, USA

ABSTRACT

To date variety of supercritical CO₂ cycles were proposed by numerous authors. Multiple small-scale tests performed, and a lot of supercritical CO cycle aspects studied. Currently, 3-10 MW-scale test facilities are being built. However, there are still several pieces of sCO₂ technology with the Technology Readiness Level (TRL) 3-5 and system modeling is one of them. The system modeling approach shall be sufficiently accurate and flexible, to be able to precisely predict the off-design and part-load operation of the cycle at both supercritical and condensing modes with diverse control strategies. System modeling itself implies the utilization of component models which are often idealized and may not provide a sufficient level of fidelity. Especially for prediction of off-design and part load supercritical CO₂ cycle performance with near-critical compressor and transition to condensing modes with lower ambient temperatures, and other aspects of cycle operation under alternating grid demands and ambient conditions.

In this study, the concept of a digital twin to predict off-design supercritical CO₂ cycle performance is utilized. In particular, with the intent to have sufficient cycle simulation accuracy and flexibility the cycle simulation system with physics-based methods/modules were created for the bottoming 15.5 MW Power Generation Unit (PGU). The heat source for PGU is GE LM6000-PH DLE gas turbine. The PGU is a composite (merged) supercritical CO₂ cycle with a high heat recovery rate, its design and the overall scheme are described in detail. The calculation methods utilized at cycle level and components' level, including loss models with an indication of prediction accuracy, are described. The flowchart of the process of off-design performance estimation and data transfer between the modules as well. The comparison of the results obtained utilizing PGU digital twin with other simplified approaches is performed. The results of the developed digital twin utilization to optimize cycle

control strategies and parameters to improve off-design cycle performance are discussed in detail.

Keywords: BOTTOMING sCO₂ CYCLE, DIGITAL TWIN, OFF-DESIGN, PART-LOAD OPERATION.

INTRODUCTION

The attempts to simulate transient and steady-state sCO₂ cycles off-design performance were performed by numerous authors [1], [2], [3], [4], and [5]. Some of them studied the dynamic behavior of regulators, some studied different control strategies or off-design behavior in different scenarios, which definitely has certain utility in the development of the reliable technology of sCO₂ cycle simulation. Nevertheless, they used rather simplified models of components, especially turbomachinery and heat exchangers, which are of crucial importance to correctly simulate cycle performance.

The authors of this paper attempted to apply the digital twin concept to a simulation of off-design and part-load modes of the sCO₂ bottoming cycle considering real machine characteristics and performance, which nobody tried to apply in this area.

On IGTC Japan 2015, SoftInWay Inc. has published a paper "Evaluation of Gas Turbine Exhaust Heat Recovery Utilizing Composite Supercritical CO₂ Cycle". The paper considered combinations of different bottoming sCO₂ cycles for a specific middle power gas turbine. It mainly studied the advantages of different types of sCO₂ cycles to increase the power production utilizing GTU waste heat.

The present paper is a further study based on that so the Cycle 2 [6] from that previous paper was selected as the sCO₂ bottoming PGU layout in the present paper for subsequent analysis. The cycle is a combination of recompression cycle and simple cycle which offers 16.13 MW as output. GE LM6000-PH DLE gas turbine, was used as the heat source for bottoming PGU. According to GE official brochure [7], the GE LM6000

offers 40 MW to over 50 MW with up to 42% efficiency and 99% fleet reliability in a flexible, compact package design for utility, industrial and oil and gas applications. GE LM6000-PH DLE provides 53.26 MW output with exhaust temperature at 471 °C and exhaust flow at 138.8 kg/s. (This information came from GE products specification from 2015. It appears that GE continuously modifying the parameters of its turbines along with the naming of different modifications. Therefore, today's parameters and configuration names might be slightly different comparing to 2015) Exhaust gas pressure was assumed to be 0.15 MPa. These parameters were taken to analyze the bottoming PGU and are presented below in TABLE 1.

TABLE 1: SELECTED SET OF GE LM6000-PH DLE PARAMETERS

Parameters	Value
GTU Thermal Efficiency	42.3 %
GTU Power	53.26 MW
Exhaust Gas Mass Flow Rate	138.8 kg/s
Exhaust Gas Temperature	471 °C
Exhaust Gas Pressure	0.15 MPa*

* The exhaust gas pressure was assigned as 0.15 MPa.

The digital twin (DT) concept is the developing technology that allows simulation of object behavior during its life cycle or in specified time due to changing ambient conditions, for example. The DT is applicable for performance tuning, digital machine building, healthcare, smart cities, etc [8] that allows decreasing the time and costs of development and optimize the object on the developing stage. GE has raised DT concepts for power plants to continually improves its ability to model and track the state of the plants [9].

In the context of this paper, DT is a simulation system comprised of physicist-based models organized in a special algorithmic structure that allows simulating the behavior of sCO₂ PGU under alternating ambient conditions and grid demands.

The DT in this study was created utilizing AxSTREAM® Platform, which includes multiple software tools. The following software tools were utilized in this study: AxCYCLE™ was used to perform cycle thermodynamic calculation; solution generator in AxSTREAM® helped with finding possible machine geometry with given boundary conditions when performing preliminary design for compressors and turbines at design point; parameters and performance of turbomachinery including mass flow rate, pressure, power, efficiencies, etc were calculated by Meanline/Streamline solver in AxSTREAM® for design and off-design conditions; AxSTREAM NET™ is a 1D system modeling solver and it was introduced here to simulate performance of heat exchangers (HEX) and pressure drop in the pipes involved in the cycle; AxSTREAM ION™ was used to integrate all modules and tools together in one simulation system.

CO₂ thermodynamic and transport properties were determined utilizing NIST RefProp [10].

1 Cycle Initial Parameterization and Simulation

The layout and preliminary parameters that were used for modeling the 16.13 MW PGU have been chosen exactly the same as Cycle 2 [6] as mentioned in the introduction. The simulated cycle of 16.13 MW PGU configuration implemented in the cycle simulation tool using NIST database property is presented in FIGURE 1.

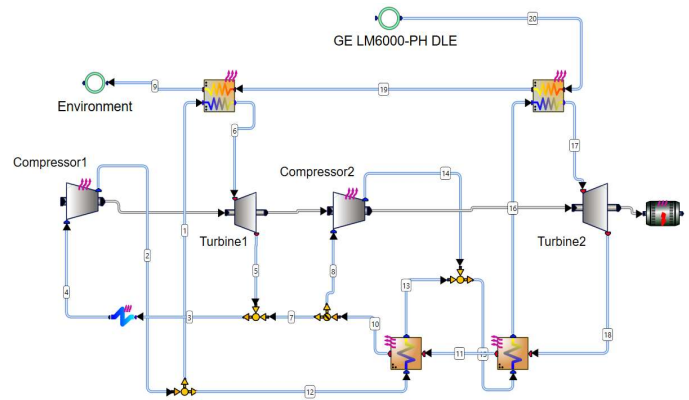


FIGURE 1: PROCESS FLOW DIAGRAM OF 16.13 MW PGU

This is a combination of a recompression sCO₂ cycle (high temperature) and a simple sCO₂ cycle (low temperature). The foundation for this combination creation was an idea to use the highly efficient recompression cycle for the high-temperature exhaust gas utilization while taking into account the rather high flue gas residual temperature after the Intermediate Heat Exchanger (IHx) of this cycle. Moreover, the recuperated cycle was installed to utilize the low-temperature exhaust fuel gas residual heat and increase the total power production. The designations which are used in FIGURE 1 and in further figures are presented in TABLE 2. Preliminary parameters taken from Cycle 2 [6] analysis are shown in TABLE 3. Values of HEX efficiency and recuperator pinch were taken from our previous paper [6]. In this study, these values were set as initial values. They were substituted with accurate values once respective components were designed. It is well known that cooler outlet temperature strongly depends on ambient conditions and even year averaged value could be different for different climates. The cooler outlet temperature was set to 33 °C as a design point and for part-load simulations. This value (or very close) is often taken as a design point value in many papers. The temperature could be set to other values depending on the climate of the anticipated location of the power system. Recompression ratio value and other cycle parameters were optimized in [6]. The optimization process and comparison with other cycles are described in [6].

Although the whole layout of the combination sCO₂ cycle was chosen to keep the same in this paper, some parameters were still under careful consideration in the next section and the cycle performance was recalculated and updated due to those changed parameters in the cycle simulation tool.

TABLE 2: THE DESIGNATIONS IN THE FIGURES FOR AXCYCLE™

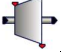
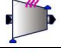

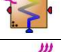


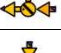
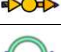

Designation	Component type
	Turbine
	Compressor
	Alternator
	Recuperator
	Intermediate Heat Exchanger (IHx)
	Cooler (heat sink)
	Control Splitter
	Mixer
	Environment or External Fluid Mass Inlet/Outlet

TABLE 3: PRELIMINARY PARAMETERS FOR SIMULATION OF THE SCO₂ CYCLE [6]

Parameter	Value
Compressor 1/Compressor 2 Efficiency	85 %
Turbine 1/Turbine 2 Efficiency	90 %
Compressors Outlet Pressure/ Turbines Inlet Pressure	28.85 MPa
Turbines Outlet Pressure	8.35 MPa
Turbine 1 Mass Flow Rate	87 kg/s
Turbine 2 Mass Flow Rate	141.5 kg/s
Turbine 1 Inlet Temperature	260.44 °C
Turbine 2 Inlet Temperature	421.68 °C
Flue Gas/CO ₂ HEX Efficiency	90 %
Pinch for CO ₂ /CO ₂ Recuperator	5 °C
Generator Efficiency	99%
Temperature at Cooler Outlet	33 °C
Recompression Ratio*	0.683
Power Output	16.13 MW

* Ratio of the mass flow rate that goes to a cooler to the mass flow rate that goes to a recompressor

2 Turbomachinery Preliminary Design and Updated Cycle Results at Design Point

The Cycle 2 [6] performance with 16.13 MW output based on some initial guess of parameters was selected as the design point of the cycle. The efficiencies for compressors and turbines were general guesses as input for Cycle 2 in the previous paper because at that stage the focus was on the performance of

different configurations of SCO₂ cycles at the design point. Details of performance for turbomachinery such as efficiencies were not considered. Besides, the pressure drop in HEXs and pipelines were ignored. In the present paper, off-design performances of the cycle at different part-load were analyzed. In order to get accurate off-design condition performance of the cycle, preliminary design for compressors and turbines were implemented. From the GTU parameters and other cycle parameters listed above, boundary conditions for compressors and turbines at design point were achieved. However, during the design process for turbomachinery, efficiency for Compressor 1 and Compressor 2 was found can't reach the value of 85 % at the same time on the same shaft. With the help of a solution generator searching for 6000 random points to get possible machine geometry solution, for constant boundary conditions, Compressor 1 is more likely to reach 80 % efficiency at a rotational speed lower than 40000 rpm. In contrast, Compressor 2 can reach higher efficiency at a rotational speed higher than 45000 rpm. The results are shown in FIGURE 2 and FIGURE 3. Each point showed in the figures refers to a different individual design and applied points are the preliminary designs of two compressors that were chosen for further study (FIGURE 4, TABLE 4 and Figure 5, TABLE 5).

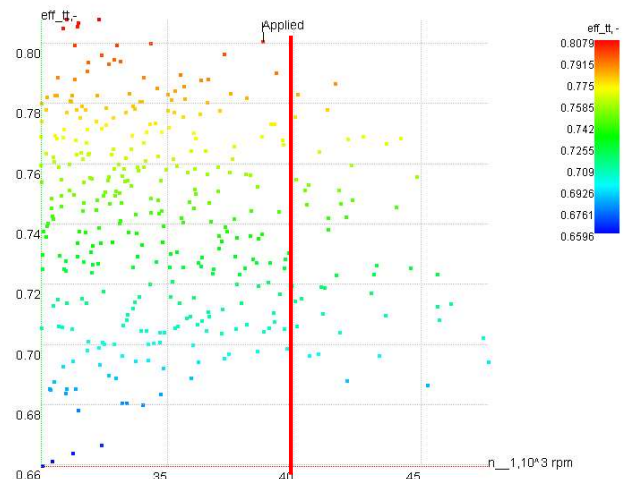


FIGURE 2: COMPRESSOR 1 RANDOM SOLUTION POINTS BY SOLUTION GENERATOR

The same rotational speed was used as a design speed for both turbines. For Turbine 2, efficiency even a little higher than 90 % can be reached. Efficiency for Turbine 1 was observed slightly lower than 90 %. Nozzle restaggering was not considered for both turbines because in the approach currently, the mass flow rate was found by given outlet pressure and the new mass flow rate was iterated back to the next iteration of calculation for cycle performance at the off-design condition. However, in later analysis, they were used to study the operation of control strategies. Preliminary design results for Turbine 1 and Turbine 2 are shown in FIGURE 6, FIGURE 7, TABLE 6 and TABLE 7.

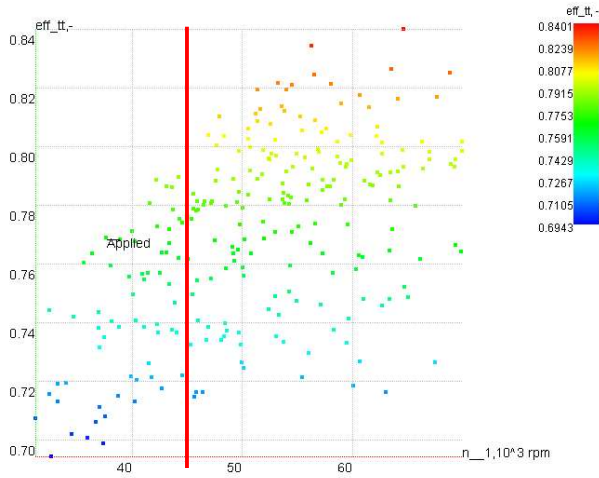


FIGURE 3: COMPRESSOR 2 RANDOM SOLUTION POINTS BY SOLUTION GENERATOR

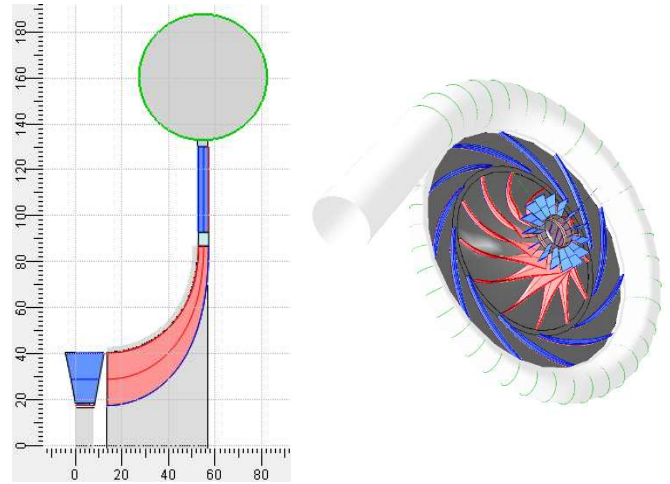


FIGURE 5: 2D AND 3D GEOMETRY VIEW OF COMPRESSOR 2

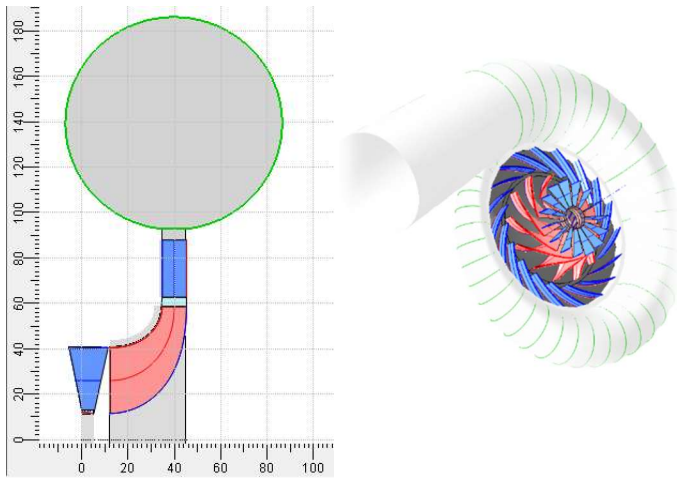


FIGURE 4: 2D AND 3D GEOMETRY VIEW OF COMPRESSOR 1

TABLE 4: PRELIMINARY DESIGN OF COMPRESSOR 1

Parameter	Value
Total Pressure at Inlet	8.35 MPa
Total Enthalpy at Inlet	296.82 kJ/kg
Total temperature at Inlet	33 °C
Static Pressure at Outlet	28.43 MPa
Total Pressure at Outlet	28.89 MPa
Mass Flow Rate at Inlet	183.65 kg/s
Rotational Speed Design Point	38000 rpm
Power	6.41 MW
Internal Total-to-total Efficiency	79.83%

TABLE 5: PRELIMINARY DESIGN OF COMPRESSOR 2

Parameter	Value
Total Pressure at Inlet	8.35 MPa
Total Enthalpy at Inlet	481.79 kJ/kg
Total temperature at Inlet	75.95 °C
Static Pressure at Outlet	28.38 MPa
Total Pressure at Outlet	28.86 MPa
Mass Flow Rate at Inlet	44.85 kg/s
Rotational Speed Design Point	38000 rpm
Power	4.09 MW
Internal Total-to-total Efficiency	78.86%

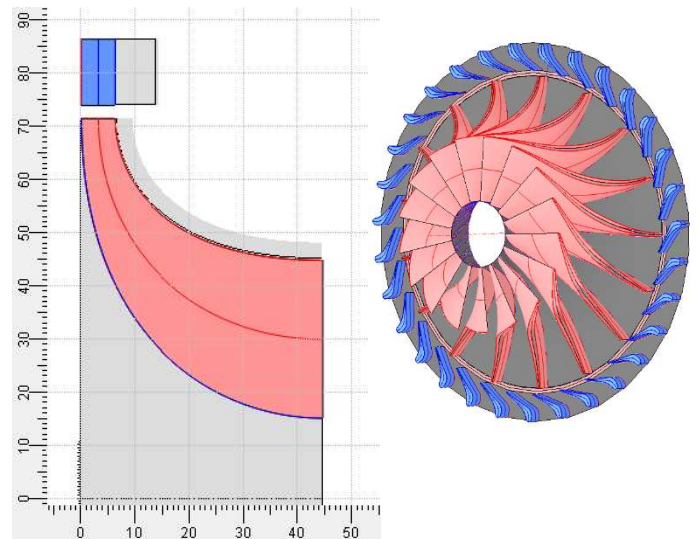


FIGURE 6: 2D AND 3D GEOMETRY VIEW OF TURBINE 1

TABLE 6: PRELIMINARY DESIGN RESULTS OF TURBINE 1

Parameter	Value
Total Pressure at Inlet	28.87 MPa

Parameter	Value
Total Enthalpy at Inlet	663.86 kJ/kg
Total Temperature at Inlet	263.92 °C
Static Pressure at Outlet	6.63 MPa
Total Pressure at Outlet	8.35 MPa
Total Temperature at Outlet	146.07 °C
Mass Flow Rate at Inlet	77.64 kg/s
Rotational Speed Design Point	38000 rpm
Power	6.86 MW
Internal Total-to-total Efficiency	89.79%

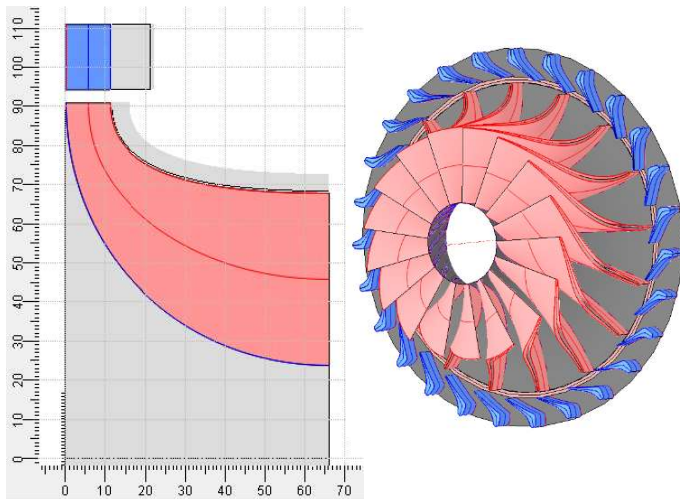


FIGURE 7: 2D AND 3D GEOMETRY VIEW OF TURBINE 2

TABLE 7: PRELIMINARY DESIGN RESULTS OF TURBINE 2

Parameter	Value
Total Pressure at Inlet	28.83 MPa
Total Enthalpy at Inlet	868.87 kJ/kg
Total Temperature at Inlet	422.59 °C
Static Pressure at Outlet	7.15 MPa
Total Pressure at Outlet	8.35 MPa
Total Temperature at Outlet	287.35 °C
Mass Flow Rate at Inlet	141.37 kg/s
Rotational Speed Design Point	38000 rpm
Power	18.56 MW
Internal Total-to-total Efficiency	91.30%

New efficiencies were defined for both compressors and turbines correspondingly in the cycle simulation tool to recalculate the PGU cycle in order to have accurate cycle performance at design point and following analysis for off-design points in the next sections. The updated cycle at design point results is presented in TABLE 8. It can be seen that with the new efficiency values the PGU power dropped from 16.13

MW to 15.5 MW. Therefore, the PGU will be referred to as a 15.5 MW unit hereafter.

TABLE 8: UPDATED PARAMETERS FOR SIMULATION OF THE SCO₂ 15.5 MW PGU CYCLE

Parameter	Value
Compressor 1 Efficiency	79.83 %
Compressor 2 Efficiency	78.86%
Turbine 1 Efficiency	89.79 %
Turbine 2 Efficiency	91.30 %
Compressors Outlet Pressure/ Turbines Inlet Pressure	28.85 MPa
Turbines Outlet Pressure	8.35 MPa
Turbine 1 Inlet Temperature	263.86 °C
Turbine 2 Inlet Temperature	422.52 °C
Turbine 1 Mass Flow Rate	87 kg/s
Turbine 2 Mass Flow Rate	141.5 kg/s
Flue Gas/CO ₂ HEX Efficiency	90%
Pinch for CO ₂ /CO ₂ Recuperator	5 °C
Generator Efficiency	99%
The temperature at Cooler Outlet	33 °C
Recompression Ratio	0.683
Power Output	15.5 MW

3 Methodology for Cycle Off-design Analysis

In an attempt to resolve the difficulties existing in off-design simulation, the main idea used in this paper is to introduce accurate simulation of turbomachinery components and heat exchangers and automate the whole process in the cycle. The entire layout of the automatic workflow shown in Figure 8. The designations which are used in FIGURE 8 and in further figures are presented in Table 9.

In the SCO₂ cycle off-design control approach, there are two primarily considered control schemes, which are bypass control and mass flow control. For the bypass control scheme, power output is controlled by changing the mass flow rate across the turbine through bypass valves. Bypass location can be anywhere within the cycle and it can deal with rapid load changes. Mass flow rate control is the most attractive control scheme for closed-cycle gas turbine power cycles to preserve efficiency with power output variations. It is usually called inventory control or pressure control (Figure 9) [11].

It should be noted that the process of withdrawal or return of the working fluid into the pipelines is transient. This process is related to a transition of the PGU from one operation mode to another. However, when the desired part-load mode was achieved and parameters stabilized the control vessel is closed, the PGU will be in steady-state. In the scope of this study, the attention was paid to steady-state modes of the PGU and thus, the transient processes as well control vessel was not considered. However, the amount of the SCO₂ in the system was evaluated

to know how much fluid is in the control vessel for each part load mode.

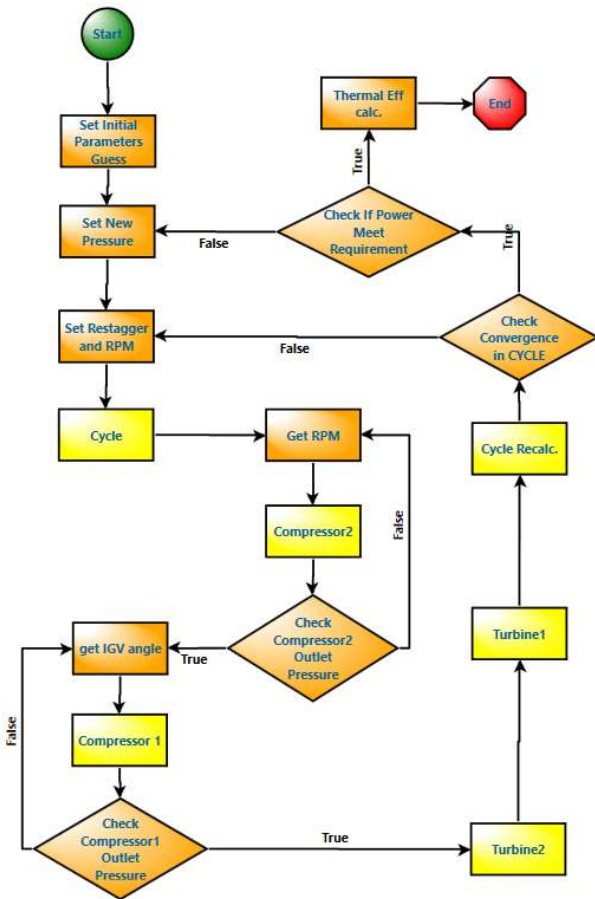


FIGURE 8: INTEGRATED AUTOMATIC WORKFLOW FOR SO2 CYCLE OFF-DESIGN ANALYSIS

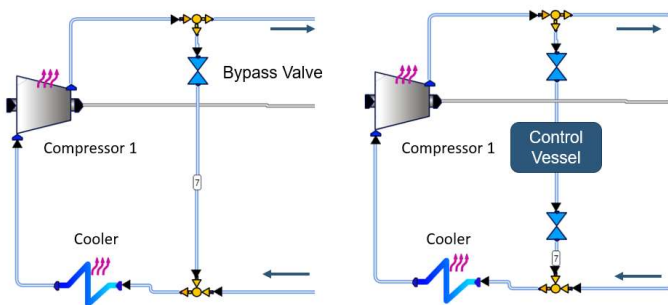





FIGURE 9 LAYOUTS OF BYPASS CONTROL (LEFT) AND MASS FLOW RATE CONTROL (RIGHT)

As mentioned, all turbomachinery components were placed on the same shaft and operated at the same rpm. The off-design behavior of compressors and turbines is different if shaft speed is varied. Therefore, even with a control vessel in the scheme, it is required to have regulating element(s) for turbomachinery, such as variable angle IGV in the compressor, variable angle nozzles in turbines, etc. The number of control elements depends

on PGU’s number of shafts and its configuration. In this study, IGV in compressor 1 was utilized as a control element to achieve the desired part-load mode. According to the chosen control scheme, the pressure at the outlet of Compressor 1 and mass flow rates of Turbine 1 and Turbine 2 was set as a variable during the off-design simulation process. These three parameters were input into the PGU cycle in cycle simulation tool to run a calculation of cycle performance for each iteration. Cycle simulation was connected to the “Cycle” block and “Cycle recal.” block. 1D/2D solver that calculates the performance for four machines were connected to the “Compressor 1” block, “Compressor 2” block, “Turbine1” block and “Turbine 2” block accordingly.

TABLE 9: THE DESIGNATIONS IN THE FIGURES FOR AUTOMATIC WORKFLOW

Picture	Meaning
	The “Script” block allows the implementation of all user technology (algorithms, process models, constraints and limitations) into the calculation process.
	The “Process” block allows connecting different tools including proprietary and commercial third-party tools via batch mode to perform joint tasks.
	The “Condition” block enables the user to perform logical operations with input parameters and proposes two scenarios of the process continuation: true or false.

For step 1, the initial guess of Compressor 1 outlet pressure, Turbine 1 and Turbine 2 mass flow rates and efficiencies of two compressors and two turbines were set to be input into cycle calculation. For step 2, PGU cycle performance was calculated for given initial guess parameters. For step 3, all sets of boundary conditions were achieved according to the last step results. Due to single-shaft configuration, the rotational speed of four machines was found by matching Compressor 2 outlet pressure to the pressure calculated from cycle simulation for step 4, with the rotational speed achieved, Compressor 1 outlet pressure was calculated. In order to match the outlet pressure with Compressor 2, the IGV restagger angle was searched for and achieved. For step 5, Turbine 1 and Turbine 2 performances were achieved for given rotational speed and mass flow rates. For step 6, with new efficiencies, outlet pressure and mass flow rates, the cycle performance was recalculated and compared with the cycle results achieved at the beginning. If they didn’t meet the convergence criteria set in the “check convergence in Cycle” block, then the workflow would go back to the “Cycle” block stage to run the next iteration calculation until the converged results achieved. For step 7, if results got converged between two cycle calculations, then the workflow went to the “Check if power meet requirement” block to check whether the power calculated from the cycle was close enough to the desired part-load power according to the criteria set in the block.

If the calculated power didn't meet the requirement, then the workflow went back to the "Set new pressure and eff" block to initialize new pressure and new efficiencies. Otherwise, the whole off-design simulation for certain part-load mode came to end. Different parameters were input for other part-load analyses with the same methodology. The binary search method was implemented in the whole workflow to quickly find the pressure, rotational speed and IGV restagger angle for a certain iteration process.

4 Cycle Off-design Simulation Results

In order to get a smooth distribution of part-load modes to study the characteristics of the off-design sCO₂ cycle, 90%, 75%, 60% and 45% of power part-load were arbitrarily chosen as the four off-design conditions to analyze in this paper. Any other part-load mode can be analyzed using this approach. According to the methodology used in the automatic workflow which was stated in the last section, initial parameters and guess values for each part-load mode were input respectively and the automatic iterating calculations were performed to simulate these four part-load modes and the results are presented in TABLE 10, TABLE 11, TABLE 12 and Table 13. It should be noted that mass flow rates and efficiencies for all components involved in this simulation were calculated according to the flow chart (Figure 8), but not set.

TABLE 10: SCO2 PGU CYCLE OFF-DESIGN PERFORMANCE RESULTS

Part-load	90%	75%	60%	45%
Power Calculated by Cycle Simulation in Automatic Workflow (MW)	13.9	11.6	9.25	6.93
Power Calculated by 1D Solver in Automatic Workflow (MW)	14.1	11.6	9.27	6.93
Deviation between 1D Solver and Cycle Simulation (%)	1.07	0.03	0.21	0.01
Desired Power (MW)	14	11.6	9.3	6.98
Deviation between Desired Power and 1D Solver (%)	0.34	0.17	0.52	0.65
Thermal Efficiency (%)	27.5	25.6	23.0	20.0

TABLE 11: TURBOMACHINE EFFICIENCY RESULTS

	Compressor 1	Turbine 1	Compressor 2	Turbine 2
Initial Efficiency Guess in Cycle Simulation	0.79	0.90	0.79	0.91
Efficiency Calculated by 1D Solver at 90% Part-load	0.81	0.88	0.78	0.90
Efficiency Calculated by 1D Solver at 75% Part-load	0.81	0.84	0.78	0.88
Efficiency Calculated by 1D Solver at 60% Part-load	0.81	0.80	0.78	0.86
Efficiency Calculated by 1D Solver at 45% Part-load	0.81	0.75	0.78	0.83

TABLE 12: ROTATIONAL SPEED AND INPUT VARIABLES RESULTS

Part-load	90%	75%	60%	45%
Rotational Speed (rpm)	35744	33027	30103	26897
Compressor1 Outlet Total Pressure (MPa)	26.39	23.6	20.99	18.37
Turbine1 MFR (kg/s)	68.48	59.07	50.89	43.30
Turbine2 MFR (kg/s)	124.89	111.35	98.7	85.79

TABLE 10 is the comparison of power values among cycle simulation, 1D solver and desired power at off-design conditions. Results from 1D solver are power values of two compressors and two turbines after the automatic process finished for each part-load. Also, thermal efficiency for the bottoming sCO₂ PGU cycle is shown in the table. The deviations among three power values are very small. For the majority of parameters, the discrepancy is less than 1 %. These deviations

can be reduced further as long as the convergence criteria are set smaller.

TABLE 11 and TABLE 12 are the results of the components involved in the cycle in off-design simulation. Efficiencies of 2 compressors almost remained the same for all four part-load modes. It was shown in the previous section that Compressor 1 and Compressor 2 have different optimal rotational speed values. The design rotational speed was found as a compromise. Thus, at certain off-design conditions, compressors' efficiency may be higher compared to a to the one at the design point. In turn, efficiencies of two turbines decreased with the output power. FIGURE 10 shows that Turbine 1 and Turbine 2 efficiencies don't decrease linearly with the reduction of the load. Besides, the efficiency of Turbine 1 dropped faster, and it dropped from 0.9 to 0.75 which means calculation with constant efficiency will lead to a large discrepancy. The normalized data of TABLE 12 is presented in FIGURE 11 below. The four parameters of components don't change exactly linearly with the part-load as well, but they are almost equidistant with each other. T1, T2, and C1 refer to Turbine 1, Turbine 2 and Compressor 1 respectively.

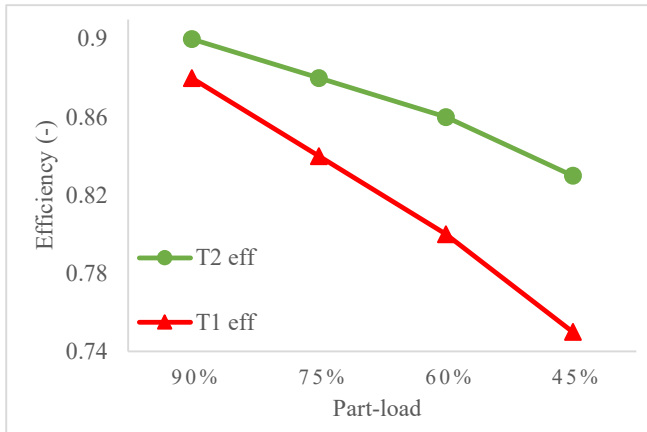


FIGURE 10: RELATION OF TURBINE 1 AND TURBINE 2 EFFICIENCIES WITH PART-LOAD

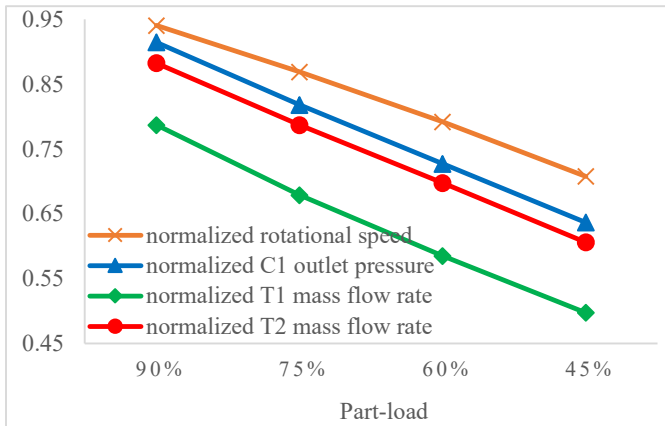


FIGURE 11: COMPONENTS NORMALIZED PARAMETERS VS PART-LOAD

TABLE 13: COMPARISON OF RESULTS FROM CYCLE SIMULATION AND AUTOMATIC WORKFLOW

	Cycle Simulation Using Constant Efficiencies	Automatic Workflow Considering Accurate Efficiencies
Compressor 1 Outlet Pressure (MPa)	24.5	26.39
Turbine 1 Mass Flow Rate (kg/s)	75	68.48
Turbine 2 Mass Flow Rate (kg/s)	124	124.89
Power (MW)	14	13.90
Cycle Thermal Efficiency (%)	24.46	27.52

(a) 90% Part-load

	Cycle Simulation Using Constant Efficiencies	Automatic Workflow Considering Accurate Efficiencies
Compressor 1 Outlet Pressure (MPa)	21.60	23.60
Turbine 1 Mass Flow Rate (kg/s)	64	59.07
Turbine 2 Mass Flow Rate (kg/s)	106	111.35
Power (MW)	11.63	11.61
Cycle Thermal Efficiency (%)	24.19	25.55

(b) 75% Part-load

	Cycle Simulation Using Constant Efficiencies	Automatic Workflow Considering Accurate Efficiencies
Compressor 1 Outlet Pressure (MPa)	21.4	20.99
Turbine 1 Mass Flow Rate (kg/s)	59.5	50.89
Turbine 2 Mass Flow Rate (kg/s)	94	98.7
Power (MW)	9.3	9.25
Cycle Thermal Efficiency (%)	21.7	23.02

(c) 60% Part-load

	Cycle Simulation Using Constant Efficiencies	Automatic Workflow Considering Accurate Efficiencies
Compressor 1 Outlet Pressure (MPa)	19.35	18.37
Turbine 1 Mass Flow Rate (kg/s)	51	43.30
Turbine 2 Mass Flow Rate (kg/s)	78	85.79
Power (MW)	6.98	6.93
Cycle Thermal Efficiency (%)	18.5	19.98

(d) 45% Part-load

5 Ambient Temperature Influence on PGU Cycle

Other than cycle off-design simulation with constant ambient temperature, due to different locations where the cycle system could be placed, lower ambient temperatures were considered in this paper to study its influence on PGU cycle performance. In order to evaluate the sensitivity of the cycle performance to the dropping ambient temperature, 18 °C and 25.5 °C were chosen as two additional cooler outlet temperatures to simulate the alternating ambient conditions. Water was used as coolant and delta temperature in cooler changed during off-design simulation. In this section, the goal was to find the maximum power for different ambient temperatures. A similar methodology was applied here as it was explained in the previous sections except that Compressor 1 outlet total pressure was kept the same as the design condition. According to previous analysis results, with a constant mass flow rate of turbines, higher pressure at compressors outlet provided higher output power. For such reason, in order to find the maximum power at different ambient temperatures, this pressure was set unchanged during the study. The results of different ambient temperatures are shown in TABLE 14.

TABLE 14: RESULTS OF CHANGING AMBIENT TEMPERATURE

Cooler Outlet T (°C)	33	25.5	18
Rotational speed (rpm)	38000	35981	34081
Compressor1 outlet total pressure (MPa)	28.85	28.85	28.85
Turbine1 MFR (kg/s)	87	82.24	77.04
Turbine2 MFR (kg/s)	141.5	138.41	136.47
Compressor 1 Efficiency (%)	79.83	79.92	80.02
Compressor 2 Efficiency (%)	78.86	76.3	77.09
Turbine 1 Efficiency (%)	89.79	89.81	87.02
Turbine 2 Efficiency (%)	91.3	89.77	88.57
Power from Automatic Workflow (MW)	15.5	15.9	15.73
Power from Cycle Simulation with Initial Guess (MW)	15.5	16.10	16.38
Thermal Efficiency from Automatic Workflow (%)	26.91	26.84	26.15

A comparison of results for two ways of cycle simulation is presented in FIGURE 12. While the ambient temperature was changing, the thermal efficiency of both off-design cases decreased slightly but both provide more power comparing to the design condition. For the traditional method, efficiencies and mass flow rates of 4 turbomachinery components were kept constant as they were at 33°C. With the accurate cycle simulation method, the cycle with temperature 25.5 °C has the highest

output power. In terms of thermodynamics, the cycle efficiency should increase with reduction of cooler temperature, which was the case when constant components efficiency cycle simulation method was used (orange curve in FIGURE 12). However, considering the influence of turbomachinery components involved in the cycle, flow rates and efficiencies changed during such a process. Power was influenced by these factors simultaneously. Moreover, the larger the difference from the cooler temperature at the design point the more significant drops the mass flow rate. The efficiency of compressor 1 altered insubstantially. However, the efficiency of compressor 2 and both turbines dropped significantly. Thus, the cycle performance continues to grow with 25.5 °C, but not so considerably compared to the simplified approach but for 18 °C the flow rate and turbomachinery performance drops so substantially, that it even surpasses the thermodynamic effect. That's the reason why automatic simulation didn't show the power increasing trend as typically anticipated with reduction of ambient temperature.

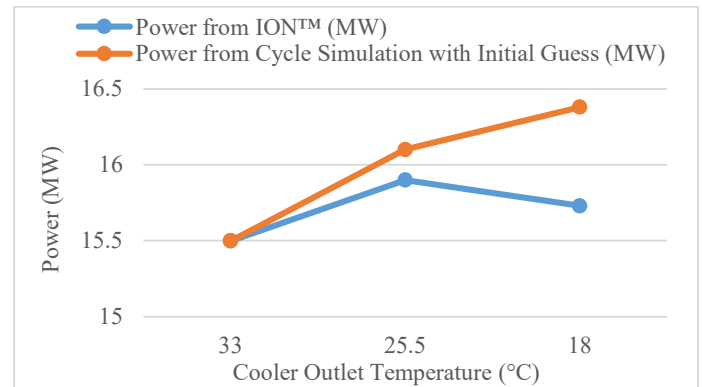


FIGURE 12: AMBIENT TEMPERATURE INFLUENCE ON CYCLES WITH INITIAL GUESS AND CYCLES CONSIDERING TURBOMACHINERY EFFICIENCIES

6 Optimization of Cycle Control Strategies

Restagger angles for both turbines were not considered in previous sections. Here different turbine restagger angles which were 0 degree, 1 degree, 2.5 degrees, -1 degree and -2.5 degree were chosen to analyze the possibility of optimizing the cycle control strategies. The variation of restagger angles of turbines had an influence on performance for the cycle and both compressors. In particular the deeper the part-load mode the smaller stability margin of compressors. This sensitivity manifests as instabilities in the operation which can lead to surge events. The same automatic methodology was applied here to study how turbine restagger angles would influence the surge margin of both compressors. Since the lower part-load mode, the closer compressors will operate to the surge line, the results of the analysis are presented for 45 % part-load mode only. The same can be easily analyzed for the other part-load modes. Here margin for surge condition was calculated by formulation below:

$$Margin = 1 - \frac{\pi}{m} * \frac{m_S}{\pi_S} \quad (1)$$

where $\pi = P_2/P_1$; P_2, P_1 = discharge and inlet pressure; m = mass flow rate; Index: s = surge;

The results are shown in TABLE 15 and FIGURE 13.

TABLE 15: TWO COMPRESSORS SURGE MARGIN WITH DIFFERENT TURBINES RESTAGGER ANGLE

Turbine Restagger Angle (degree)	Compressor 1 Surge Margin (%)	Compressor 2 Surge Margin (%)
2.5	19.73	0.06
1	24.87	4.77
0	24.32	5.14
-1	25.06	10.00
-2.5	26.81	16.92

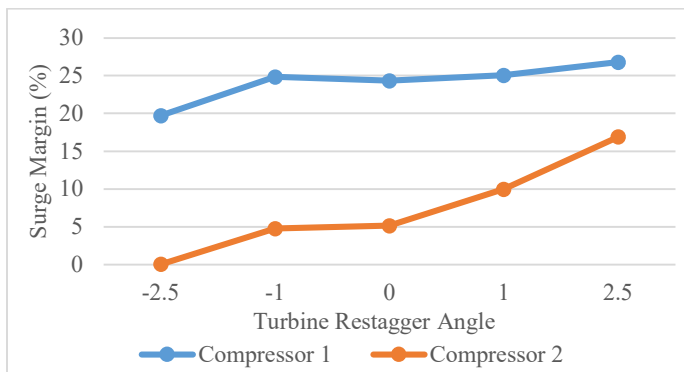


FIGURE 13: TWO COMPRESSORS SURGE MARGIN WITH DIFFERENT TURBINES RESTAGGER ANGLE

Both compressors surge margin increased with restagger angles decreasing. Compressor 2 operated very close to the surge limit at the initial operating conditions. Also, the surge margin of Compressor 2 is more sensitive to turbines restagger angles than Compressor 1. In order to operate the cycle safely, some negative value of the turbine restagger angle is necessary and important. This is important information, which can be used to correctly select the respective turbine restagger angle or even make a decision about the compressor 2 redesign.

The present paper emphasized on the overall cycle performance and characteristics at off-design conditions. A more detailed analysis of turbomachinery components involved in such a cycle will be performed in a future.

7 HEXs and Pipelines Simulation and Updated Cycle Off-design Analysis

The simple thermodynamic scheme of a power plant is drawn up at the initial stage of designing. An analysis of the off-design operating modes of this unit using such a simplified scheme is possible. However, at the same time, a number of assumptions are laid in the calculation, most often are like these:

- The absence of hydraulic losses in the network and heat exchangers or the setting of these losses as constant.
- Constant effectiveness of heat exchangers.

Such assumptions may lead to serious calculation discrepancies including insufficient power of the designed unit or the inability to provide one of the off-design modes. Therefore, the critical task of the most accurate calculation of the entire system as a whole, taking into account the real characteristics of the equipment and network. Later in the paper it will be shown how the above assumptions regarding the hydraulic network and heat exchangers can affect the actual operating parameters of the unit. To more accurately take into account hydraulic resistance and heat exchange in the unit elements, we used the 1D thermo-hydraulic solver AxSTREAM NET™. The network simulated in this way can be combined with the accurate calculation of compressors and turbines in 1D solver in the batch mode which is very similar to what was done in previous sections. To build a refined scheme, 2 stages were performed:

- Heat exchangers, the layout of the system and connecting pipelines design and optimization
- Detailed modeling of the network as a whole in the 1D solver.

Microtubular heat exchangers were chosen as heaters. Such heat exchangers can withstand the large pressure differences that exist between supercritical CO₂ and flue gases. PCHE heat exchangers with direct channels and cross-flow fluids were chosen as regenerators and coolers. The main advantages of this type of heat exchangers are compactness (which is important for sCO₂ cycles due to small heat transfer coefficients) and low hydraulic resistance. FIGURE 14 shows the unit network modeled in 1D hydraulic solver. The updated automatic workflow for cycle off-design simulation is shown in FIGURE 15.

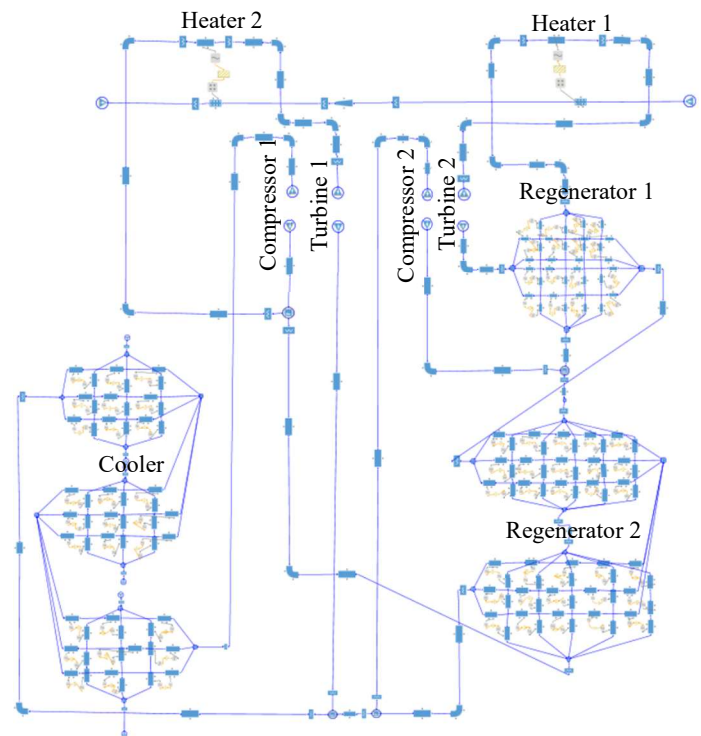


FIGURE 14: HEXS AND PIPES NETWORK SIMULATION

Following models for calculating heat transfer coefficients were used for simulating heat transfer in 1D solver:

- Inside the tubes of a microtubular heat exchanger - the Petukhov-Kirillov equation [12];
- Outside the microtubular heat exchanger tubes - Isachenko equation [13];
- In the channels of the PCHE heat exchanger - Glinsky correlation [11].

When modeling hydraulic resistance next models were used:

- Inside the microtubular heat exchanger tubes and inside the PCHE heat exchanger channels - the equation for calculating the hydraulic resistance for supercritical CO₂ [14];
- Outside the microtubular heat exchanger tubes [15].

around 87% of the max power achieved in previous analysis with cycle simulation.

The comparison of the two simulation results is shown in the charts below (FIGURE 16, FIGURE 17). The substantial variation of pressure drops in heat exchangers is presented in FIGURE 18.

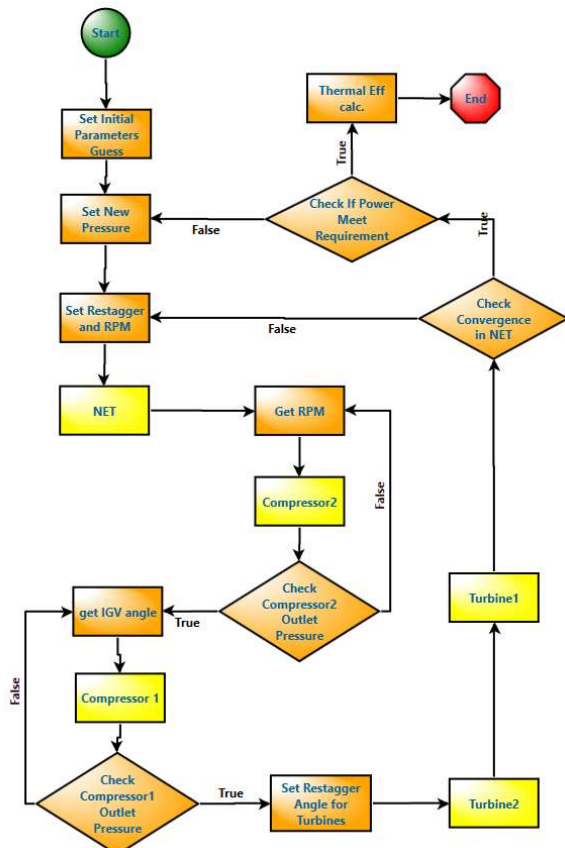


FIGURE 15: AUTOMATIC WORKFLOW WITH HYDRAULIC MODELING REPLACING CYCLE THERMODYNAMIC SIMULATION

The mechanical design procedure for PCHR design is given in reference [16]. Interval calculation of heat exchangers made it possible to most accurately take into account the variable parameters of the fluids and the flow directions inside the apparatus.

The methodology used here was almost the same as the one used in previous sections. The difference is that the 1D hydraulic simulation block replaced the cycle thermodynamic simulation block in the automatic process. Due to considering actual losses of HEXs and pipes, the max power that could be achieved was

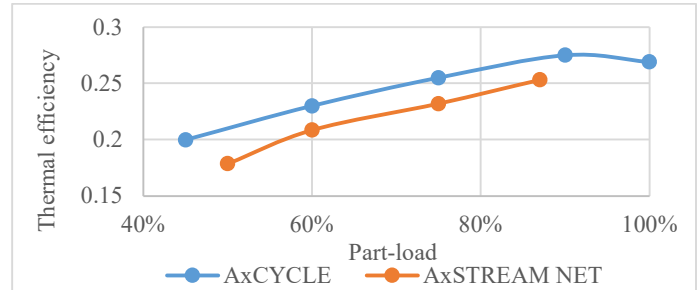


FIGURE 16: COMPARISON OF CYCLE THERMAL EFFICIENCY AT DIFFERENT PART-LOAD MODES

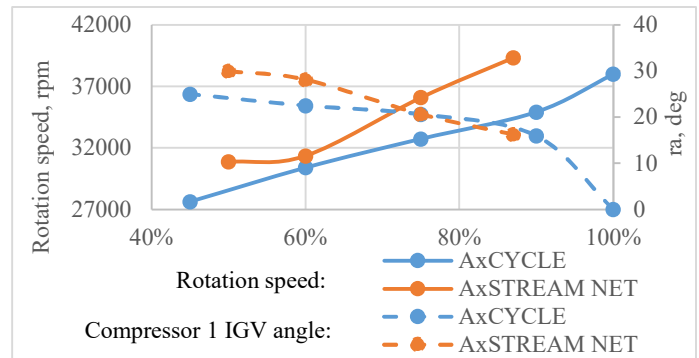


FIGURE 17: COMPARISON OF TURBOMACHINERIES RPM AND IGV ANGLE AT DIFFERENT PART-LOAD MODES

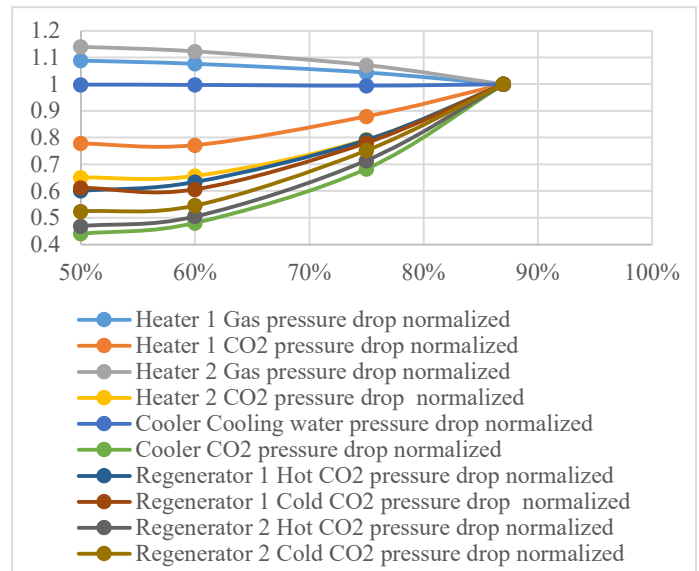


FIGURE 18: NORMALIZED PRESSURE DROPS IN HEXS VS LOAD

CONCLUSION

- The automatic process connecting different tools for off-design analysis to get accurate results of cycle and turbomachinery performance was introduced and explained in detail. It gave us high accuracy and flexibility to run off-design analysis for such kind of sCO₂ bottoming PGU cycle rapidly.
- Results of cycle simulation with constant initial guess efficiencies of turbomachinery and results of cycle simulation considering real efficiencies at different part-load modes which are 90%, 75%, 60%, and 45% were compared and significant discrepancies are presented, demonstrating the importance of accurate determination of components performance.
- The influence of lower ambient temperature on the sCO₂ cycle was studied. 25.5 °C and 18 °C were chosen as two different cooler outlet temperature to study changing ambient conditions. 25.5°C case showed that cycle provided the highest output power due to counter effects of turbomachinery efficiency and overall cycle thermodynamics. This effect was not caught by conventional cycle simulation approach.
- The optimization of sCO₂ cycle control strategies was discussed. Without turbines restagger angle, current design for Compressor 2 operated very close to surge limit. Also Compressor 2 showed more sensibility to turbine restagger angle than Compressor 1. This is important information, enables the possibility to correctly select the respective turbine restagger angle or even make a decision about the compressor 2 redesign.
- 1D system network modeling tool was introduced into the original methodology in order to simulate pressure drop and losses in HEXs and pipelines. Max output power decreased due to the consideration of hydraulic losses. Therefore, in order to be able to produce the desired power it is required to redesign the turbomachinery components taking into account PGU off-design performance including hydraulic network.
- The developed digital twin of the bottoming sCO₂ generation power unit allowed to rapidly simulate off-design and part-load modes and reveal multiple crucial aspects to be considered during the design phase, which was impossible with conventional cycle simulation approaches.

ACKNOWLEDGEMENTS

We wish to thank the many people from SoftInWay Inc. team who generously contributed their time and effort in the preparation of this work. The strength and utility of the material presented here are only as good as the inputs. Their insightful contributions are greatly appreciated.

REFERENCES

- [1] C. Gao, P. Wu, J. Shan and B. Zhang, "Development of A Transient Analysis Code for S-CO₂ Power Conversion System," in *The 6th International Supercritical CO₂ Power Cycles Symposium*, Pittsburgh, Pennsylvania, 2018.
- [2] P. Mahapatra, J. Albright, S. Zitney and E. Liese, "Advanced Regulatory Control of a 10 MWe Supercritical CO₂ Recompression Brayton Cycle towards Improving Power Ramp Rates," in *The 6th International Supercritical CO₂ Power Cycles Symposium*, Pittsburgh, Pennsylvania, 2018.
- [3] M. Huang, C.-J. Tang and A. McClung, "Steady State and Transient Modeling for the 10 MWe sCO₂ Test Facility Program," in *The 6th International Symposium Supercritical CO₂ Power Cycles*, Pittsburgh, Pennsylvania, 2018.
- [4] S. A. Wright, C. S. Davidson and C. Husa, "Off-design performance modeling results for a supercritical CO₂ waste heat recovery power system," in *The 6th International Supercritical CO₂ Power Cycles Symposium*, Pittsburgh, 2018.
- [5] T. A. Louis and N. Ty, "ANALYSIS AND OPTIMIZATION FOR OFF-DESIGN PERFORMANCE OF THE RECOMPRESSION sCO₂ CYCLES FOR HIGH TEMPERATURE CSP APPLICATIONS," in *The 5th International Symposium – Supercritical CO₂ Power Cycles*, San Antonio, 2016.
- [6] L. Moroz, M. Burlaka, O. Rudenko and C. Joly, "Evaluation of Gas Turbine Exhaust Heat Recovery Utilizing Composite Supercritical CO₂ Cycle," 2015.
- [7] "Fast, Flexible Power Aeroderivative Product and Service Solutions," [Online]. Available: https://www.ge.com/content/dam/gepower-pgdp/global/en_US/documents/product/aeroderivative-products-services-brochure.pdf.
- [8] N. Joshi, "Applications of digital twin," [Online]. Available: <https://www.allerin.com/blog/applications-of-digital-twin>.
- [9] GE, "GE Digital Twin Analytic Engine for the Digital Power Plant," [Online]. Available: https://www.ge.com/digital/sites/default/files/download_assets/Digital-Twin-for-the-digital-power-plant-.pdf.
- [10] NIST, "REFPROP," NIST, [Online]. Available: <https://www.nist.gov/srd/refprop>.
- [11] V. Dostal, M. Driscoll and P. Hejzlar, A Supercritical Carbon Dioxide Cycle for Next Generation Nuclear Reactors, 2004.
- [12] Petukhov, Heat Transfer in Nuclear Power Plants, 1974.
- [13] Orlov, Theoretical Foundations of Heat Engineering. Heat and Mass Transfer, 2013.
- [14] Z. Wang, B. Sun, J. Wang and L. Hou, "Experimental Study on The Friction Coefficient of Supercritical Carbondioxide In Pipes," in *International Journal of Greenhouse Gas Control* 25, 2014.
- [15] Bazhan, Kanevets and Selivestrov, Handbook of Heat Exchangers, 1989.
- [16] R. L. Pierres, D. Southall and S. Osborne, "Impact of Mechanical Design Issues on Printed Circuit Heat Exchangers," in *Heatric Division of Meggitt (UK) Ltd. Proceedings of sCO₂ Power Cycle Symposium*, 2011.